

Large Eddy Simulation of Compartment Fire with Gas Combustible

Mliki Bouchmel, Abbassi Mohamed Ammar, Kamel Geudri, Chrigui Mouldi, Omri Ahmed

Abstract—The objective of this work is to use the Fire Dynamics Simulator (FDS) to investigate the behavior of a kerosene small-scale fire. FDS is a Computational Fluid Dynamics (CFD) tool developed specifically for fire applications. Throughout its development, FDS is used for the resolution of practical problems in fire protection engineering. At the same time FDS is used to study fundamental fire dynamics and combustion. Predictions are based on Large Eddy Simulation (LES) with a Smagorinsky turbulence model. LES directly computes the large-scale eddies and the sub-grid scale dissipative processes are modeled. This technique is the default turbulence model which was used in this study. The validation of the numerical prediction is done using a direct comparison of combustion output variables to experimental measurements. Effect of the mesh size on the temperature evolutions is investigated and optimum grid size is suggested. Effect of width openings is investigated. Temperature distribution and species flow are presented for different operating conditions. The effect of the composition of the used fuel on atmospheric pollution is also a focus point within this work. Good predictions are obtained where the size of the computational cells within the fire compartment is less than 1/10th of the characteristic fire diameter.

Keywords—Large eddy simulation, Radiation, Turbulence, combustion, pollution.

I. INTRODUCTION

As a basic phenomenon, combustion has always attracted attention throughout fire research history. A lot of investigators have contributed to the fire combustion research with well-designed experiments: among them [1]-[8]. With the increase of computational power and numerical methods, more research work shifted to the numerical simulation of fire combustion. The need for improvement in predicting flame heat flux, an alternative combustion model has been realized in the code by [9]. The combustion model was based on infinitely fast chemistry and mixture fraction formalism.

M. Bouchmel is with the Unité de recherche : Matériaux, Energie et Energies Renouvelables (MEER), Faculté des Sciences de Gafsa, BP : 19, Zarroug, 2112, Gafsa, Tunisie (phone: 21626894606; e-mail: mlikibouchmel@yahoo.fr).

A. Mohamed Ammar is with the Unité de recherche : Matériaux, Energie et Energies Renouvelables (MEER), Faculté des Sciences de Gafsa, BP : 19, Zarroug, 2112, Gafsa, Tunisie (e-mail: abbassima@gmail.com).

C. Mouldi is with the Unité de recherche : departement of Mechanical Engineering, Institute for Energy and Powerplant Technology, Technische Universität Darmstadt, Patersenstrasse 30, D-64287 Darmstadt, Germany (e-mail: mechrigui@ekt.tu-darmstadt.de).

G. Kamel is with the Mechanical Engineering Department, College of Engineering and Islamic Architecture, Umm Al-Qura University, KSA (e-mail: kamelgeudri@yahoo.fr).

O. Ahmed is with the Unité de recherche : Matériaux, Energie et Energies Renouvelables (MEER), Faculté des Sciences de Gafsa, BP : 19, Zarroug, 2112, Gafsa, Tunisie (e-mail: ahom206@yahoo.fr).

As a basic phenomenon, combustion has always attracted attention throughout fire research history. A lot of investigators have contributed to the fire combustion research with well-designed experiments: among them [1], [4], [10]. With the increase of computational power and numerical methods, more research work shifted to the numerical simulation of fire combustion. The need for improvement in predicting flame heat flux, an alternative combustion model has been realized in the code by Kennedy [9]. The combustion model was based on infinitely fast chemistry and mixture fraction formalism.

This paper is an extension of the vassilly works that studies the phenomenon of the combustion in compartment of fire [10]. The combustion model is implemented in Fire Dynamics Simulator (FDS) [11], [12]. The code, Fire Dynamics Simulator (FDS), including its visualization tool (Smokeview), is a very promising research tool for fire investigation [16], [17]. It is based on Large Eddy Simulation (LES) with Smagorinsky turbulence sub-model. This technique is used by FDS to model the dissipative processes (viscosity, thermal conductivity, and material diffusivity) that occur to the smaller scales [11], [14]. In order to validate this new model for general applications in fire growth, it was decided to investigate the kerosene fire since it has many industrial applications. First comparisons between the numerical and experimental results of the kerosene fires are presented. Then, the effect of the composition of the fuel used on the atmospheric pollution is investigated. Finally, thermal loss effect of the walls on the temperature inside and outside the fire compartment for two different values of the thermal conductivity are analyzed.

II. MODELING APPROACHES

A. Governing Equations

The filtered conservation equations for mass, momentum and energy for a Newtonian fluid are solved. A particularly useful reference for a description of these equations, the notation used, and the various approximations employed is given by [15].

Mass conservation

$$\frac{\partial \rho}{\partial t} + \nabla \cdot \rho \mathbf{v} = 0 \quad (1)$$

Momentum conservation

$$\frac{\partial (\rho \mathbf{v})}{\partial t} + \nabla \cdot (\rho \mathbf{v} \mathbf{v}) + \nabla (p) = \mathbf{f} \rho + \nabla \cdot \boldsymbol{\tau}_{ij} \quad (2)$$

Energy conservation

$$\frac{\partial(\rho h)}{\partial t} + \nabla \cdot (\rho h \mathbf{v}) = \frac{Dp}{Dt} + \dot{q}''' - \nabla \cdot \mathbf{q} + \Phi \quad (3)$$

Species diffusion

$$\frac{\partial \rho Y_i}{\partial t} + \nabla \cdot (\rho Y_i \mathbf{v}) = -\nabla \cdot \mathbf{J}_i + \dot{m}_i''' \quad (4)$$

where ρ , $\mathbf{v}(u, v, w)$, p , and h denote the density, the three components of velocity \mathbf{v} , the pressure and enthalpy, respectively. The term $\nabla \cdot \mathbf{q}$ represents the divergence of the conductive and radiative heat flux. The term Φ is known as the dissipation function, the rate at which kinetic energy is transferred to thermal energy due to the viscosity of the fluid.

B. Turbulence Model

Details of the hydrodynamics and turbulence model are supplied in [16]. Following the analysis of Smagorinsky [11], the viscosity μ_{LES} is modeled by the following equation:

$$\mu_{LES} = \rho (C_s \Delta)^2 \left((2\bar{S}_{ij} \cdot \bar{S}_{ij}) - \frac{2}{3} (\nabla \bar{v})^2 \right)^{\frac{1}{2}} \quad (5)$$

The diffusive parameters, the thermal conductivity and material diffusivity are related to the turbulent viscosity by:

$$k_{LES} = \frac{\mu_{LES} C_p}{Pr} \quad (6)$$

$$(\rho D)_{I,LES} = \frac{\mu_{LES}}{Sc} \quad (7)$$

The Prandtl number (Pr) and the Schmidt number (Sc) are assumed to be constant and equal to 0.7.

C. Combustion Model

FDS uses the mixture fraction model as the default combustion model [16]. The mixture fraction is a conserved scalar quantity. The combustion model used here is based on mixture-fraction infinitely fast chemistry kinetics. The general form of the combustion reaction is



The mixture fraction Z is defined as in [15].

$$Z = \frac{s Y_F - (Y_{O_2} - Y_{O_2}^\infty)}{s Y_F + Y_{O_2}^\infty}, \quad s = \frac{v_{O_2} M_{O_2}}{v_F M_F} \quad (9)$$

Z varies between 1 in a region containing only fuel and $Z=0$ where the oxygen mass fraction takes its depleted ambient value $Y_{O_2}^\infty$ (Fig. 1). Note that Y_F^1 is the fraction of fuel in the fuel stream. The quantities M_F and M_{O_2} are the fuel and oxygen molecular weights, respectively. In its traditional implementation, mixture fraction chemistry assumes that fuel and oxygen cannot co-exist. That is, it uses an infinite reaction rate and assumes that fuel and oxygen will react at any temperature. The mixture fraction satisfies the conservation law [16]:

$$\rho \frac{DZ}{Dt} = \nabla \cdot (\rho D) \nabla Z \quad (10)$$

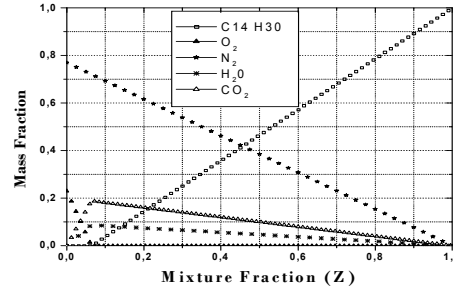


Fig. 1 Curves of balance for the case of kerosene in the hypothesis of an infinitely fast chemistry

The assumption that the chemistry is ‘‘fast’’ means that the reactions that consume fuel and oxidizer occur so rapidly that the fuel and oxidizer cannot co-exist. The flame sheet is the location where fuel and oxidizer vanish simultaneously:

$$Z(x, t) = Z_f \quad Z_f = \frac{Y_{O_2}^\infty}{s Y_F^1 + Y_{O_2}^\infty} \quad (11)$$

This leads to the ‘‘state relation’’ between the oxygen mass fraction Y_{O_2} and the mixture fraction:

$$Y_{O_2}(Z) = \begin{cases} Y_{O_2}^\infty (1 - \frac{Z}{Z_f}) & Z < Z_f \\ 0 & Z > Z_f \end{cases} \quad (12)$$

The heat release rate per unit volume is based on [18] of oxygen consumption, where ΔH_{O_2} is assumed constant for most fuels.

$$\dot{q}''' = \Delta H_{O_2} \dot{m}'''_{O_2} \quad (13)$$

Combined with the radiant heat loss, the heat release rate is then put back to the conservation equation of energy (3) to calculate the temperature and other flow variables.

The fraction of fuel mass converted into carbon monoxide, is linked to the soot yield:

$$y_{CO} = 0.0014 \frac{12x}{M_{FVF}} + 0.37 y_s \quad (14)$$

where x is the number of carbon atoms in a fuel molecule and MF is the molecular weight of the fuel.

D. Radiation and Soot

The radiation model by Anderson [11] is used in FDS. It solves the finite-volume-based radiation transport equations [13] and considers soot as the most important combustion product controlling the thermal radiation from the fire and hot smoke. Details of the radiation model are given in [11]. The Radiative Transfer Equation (RTE) for an absorbing/emitting and scattering medium is

$$d\Omega' s \cdot \nabla I_\lambda(x, s) = -(k(x, \lambda) + \sigma_s(x, \lambda))I(x, s) + B(x, \lambda) + \frac{\sigma_s(x, \lambda)}{4\pi} \int_{4\pi} \Phi(s, s') I_\lambda(x, s') \quad (15)$$

where $I_\lambda(x, s)$ is the radiation intensity at wavelength λ , s is the direction vector of the intensity, $k(x, \lambda)$ and $\sigma_s(x, \lambda)$ are the local absorption and scattering coefficients, respectively, and $B(x, \lambda)$ is the emission source term. In the case of a non-scattering gas the RTE becomes

$$s \cdot \nabla I_\lambda(x, s) = k(x, \lambda)(I_b(x)) - I_\lambda(x, s) \quad (16)$$

where $I_b(x)$ is the source term given by the Planck function. This section describes the radiation transport in the gas phase. The divergence of the radiative heat flux is given by the following equation

$$-\nabla \cdot q_x = k(x)(U(x) - 4\pi I_b(x)) \quad ; \quad \text{where } U(x) = \int_{4\pi} I(x, s) d\Omega. \quad (17)$$

The net radiant energy gained by a grid cell is the difference between the absorption and emission. The source term is defined as:

$$kI_b = \begin{cases} \frac{k\sigma T^4}{\pi} \rightarrow \text{Outside} \\ \frac{\chi_r \dot{q}'''}{4\pi} \rightarrow \text{Inside} \end{cases} \quad (18)$$

Here \dot{q}''' is the chemical heat release rate per unit volume and χ_r is the local fraction of the energy emitted as thermal radiation. The radiant heat flux vector q_x is

$$q_x = \int_{4\pi} x I(x, s) d\Omega \quad (19)$$

In the simulations, the default parameters for radiation calculation are used since no better experimental result on radiation prediction in flames are available.

III. RESULTS AND DISCUSSION

The experimental results [19] are used for the validation of the calculation code in the kerosene flame in interaction with a wall. The general arrangement of the experimental stand is illustrated in Fig. 2. The dimensions of the fire compartment are $(1.2 \times 1.0 \times 0.82) \text{ m}^3$ with a door opening of $(0.28 \times 0.56) \text{ m}^2$ in the middle of the front wall. The fire source is positioned in the center of the compartment at 0.08 m height. A complete description is provided in [19]. The thermocouples are placed inside the compartment fire, with coordinates shown in Figs. 4, 5. Geometrical dimensions of the experimental stand are shown in Fig. 3.



Fig. 2 Studied installation

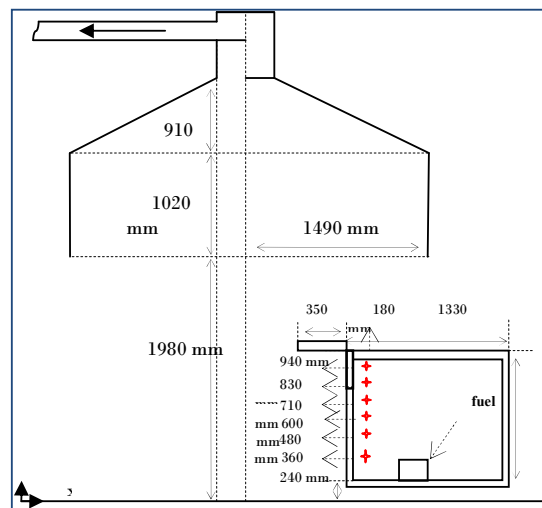


Fig 3 Longitudinal section

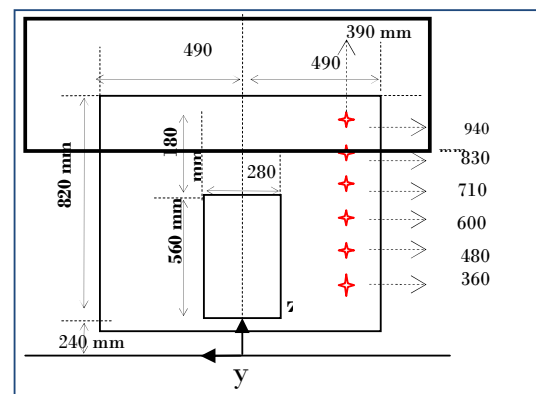


Fig. 4 The front view: Positions of thermocouples

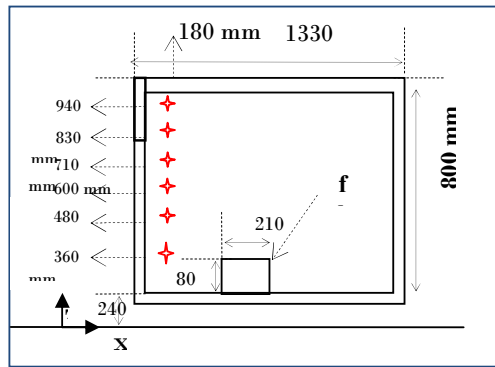


Fig. 5 Longitudinal section: Positions of thermocouples

A. Simulation Domain and Grid Size

Fig. 6 shows the compartment geometry as a 'Smokeview' picture. A computational domain 5m wide by 5m long by 5.2 m high was used for FDS simulation of the kerosene combustion region and propagation of smoke to the exit of the fire compartment. An open boundary condition was specified in the middle of the front wall of the fire compartment to allow a free flow of air into the domain. An illustration showing the grid is given in Fig. 7.

Temperatures are measured with six thermocouples placed inside the compartment of fire (Fig. 2). The six thermocouples are positioned on the following locations TA ($x_1=68\text{cm}$, $y_1=-39\text{cm}$, $z_1=94\text{cm}$), TB ($x_1=68\text{cm}$, $y_1=-39\text{cm}$, $z_1=83\text{cm}$), TC ($x_1=68\text{cm}$, $y_1=-39\text{cm}$, $z_1=71\text{cm}$), TD ($x_1=68\text{cm}$, $y_1=-39\text{cm}$, $z_1=60\text{cm}$), TE ($x_1=68\text{cm}$, $y_1=-39\text{cm}$, $z_1=48\text{cm}$), TF ($x_1=68\text{cm}$, $y_1=-39\text{cm}$, $z_1=36\text{cm}$). The total temperature in compartment fire is the arithmetic average of the six local measured temperatures on compartment fire. Inside the reservoir of smoke three thermocouples are set at: TA ($x_1=0\text{cm}$, $y_1=0\text{cm}$, $z_1=200\text{cm}$), TB ($x_1=0\text{cm}$, $y_1=-30\text{cm}$, $z_1=200\text{cm}$), TC ($x_1=0\text{cm}$, $y_1=-60\text{cm}$, $z_1=200\text{cm}$). The external temperature is set to $T_{\text{ex}}=14\text{C}^\circ$ [19]. Fig. 8 shows the comparison of the predicted mean temperature distributions inside the reservoir of smoke using three different grid resolutions, the coarse grid ($25 \times 25 \times 42$), the medium grid ($50 \times 50 \times 64$) and the fine grid ($72 \times 72 \times 64$). The predictions with the coarse grid show largest discrepancies with the experimental data. The predictions using the fine grid, as employed in the present study, are the closest to the experimental results by Piotr Smardz and Novozhilov [19], while the predictions using the medium grid are reasonably close to that of the fine grid and the experimental data. The computation time of the three cases are listed in Table I.

TABLE I
TIME OF SIMULATION

	Grid size	Time (h)
CAS 1	$25 \times 25 \times 42$	17.31
CAS 2	$50 \times 50 \times 64$	24.7
CAS 3	$72 \times 72 \times 64$	43.84

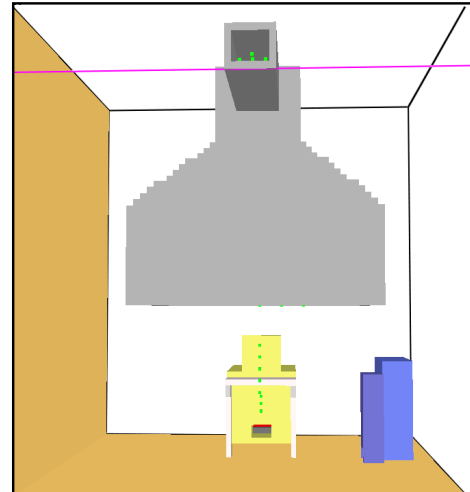


Fig. 6 Compartment geometry as a 'Smokeview' picture

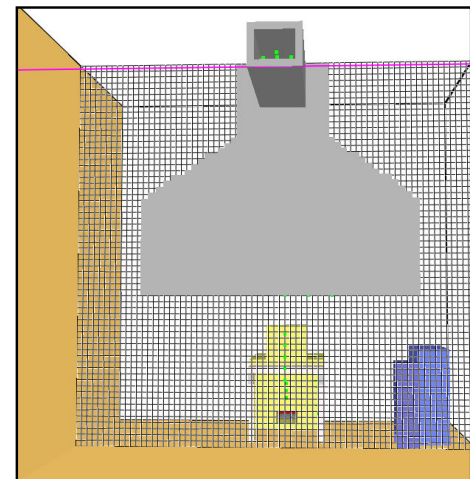


Fig. 7 Grid size

Hence the fine grid is chosen for the present study. One notes that the difference between the simulated temperature and the experimental values in an interval of time between 400 and 500 seconds are important. Fig. 9 shows that the agreement between prediction and measures are less good for the profile of middle temperature inside the compartment fire. This is probably because of the difficulty appraising the thermal fluxes correctly to the wall. This difference may be originated from the particle deposition on the thermocouples sensor. It can be retrieved that the precision of predictions of the temperature by the code FDS depends greatly on the resolution grid.

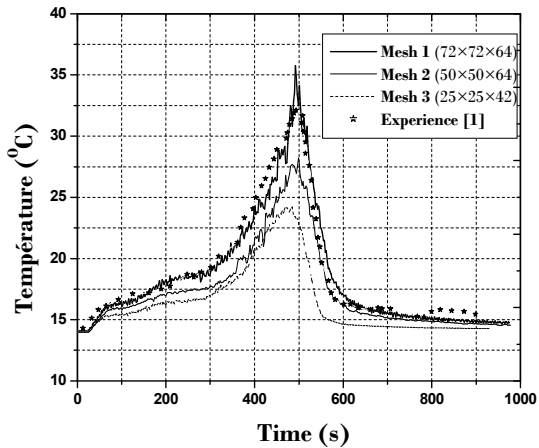


Fig. 8 Effect of the mesh resolution on the temperature profile of the middle inside reservoir of smoke

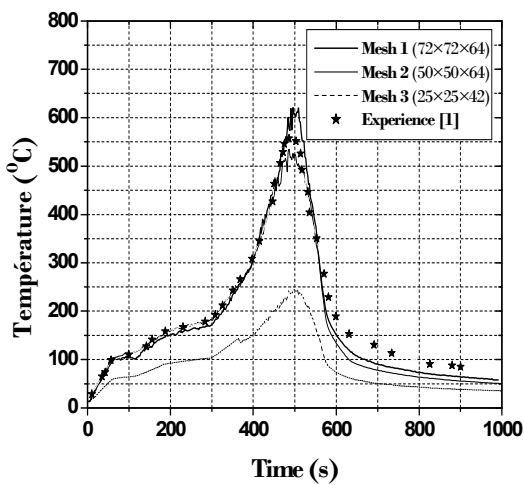


Fig. 9 Effect of the mesh resolution on the profile of the temperature inside the compartment of fire

B. Temperature Profiles inside the Compartment Fire

The compared variables are temperature evolution in different locations and the Heat Rate Release (HRR) during the combustion. Temperatures in Figs. 10, 11 correspond to positions inside the fire compartment, T_A ($x_A=680\text{mm}$, $y_A=-390\text{mm}$, $z_A=940\text{mm}$) and T_E ($x_D=680\text{mm}$, $y_D=-390\text{mm}$, $z_D=480\text{mm}$) (see Fig. 10). The measurements of Vasily Novozhilov are also presented in the same figures. One notices the important difference between the simulations and the experimental data within the interval of time 400 and 500 seconds for (T_A) (Fig. 11). This difference can be caused by the deposition of particles on thermocouples. In addition, thermocouples introduced in the compartment disturb the outflow. Results given by the code are in good agreement with the mean value of the measured temperatures. Fig. 12 shows a good agreement between predictions and measures for the temperature profile at the level (TE). This agreement reveals that the quantity of soot at the bottom part of the fire compartment is decreased. Fig. 13 shows a comparison between input heat rate release and the calculated value, the

two curves demonstrate similar profiles. The difference between the experimental results and FDS predictions may be caused by the fact that thermocouples inside the compartment are covered by a thick layer of soot that is produced by the combustion of the fuel used.

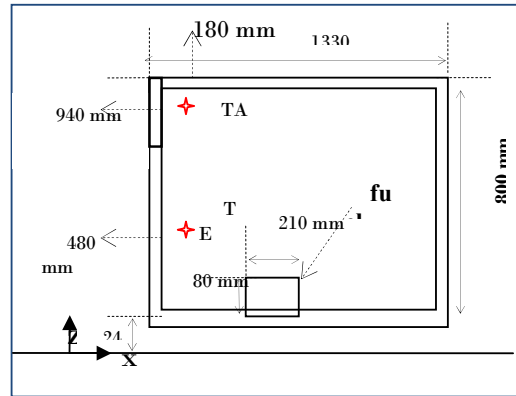


Fig. 10 Positions of thermocouples (T_A , T_D)

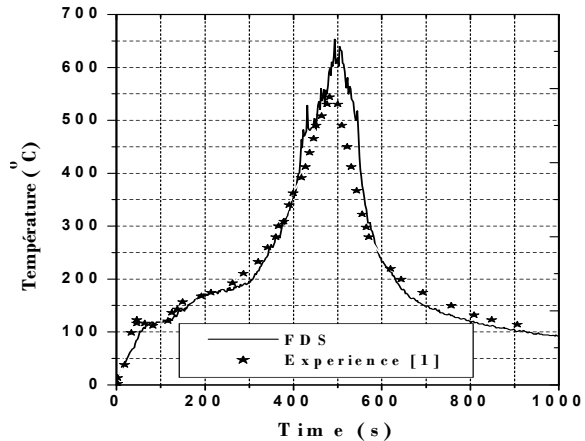


Fig. 11 Temperature profile $z=940\text{mm}$

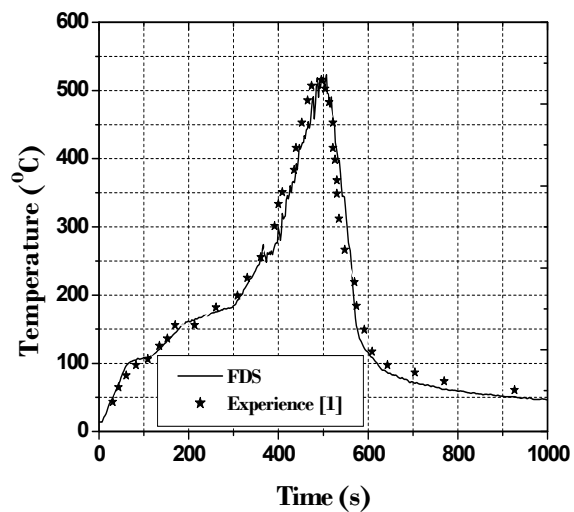


Fig. 12 Temperature profile $z = 480\text{mm}$

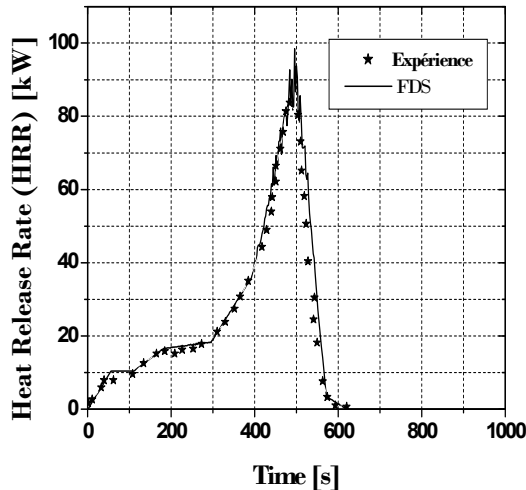


Fig. 13 Heat Rate Release (HRR)

C. Effect of the Opening Size

Five numerical simulations were made to investigate the effect of the opening size on gas temperature profiles in compartment fire. Five different aspect ratio of openings ($L=0.03$; 0.12 ; 0.20 ; 0.28 and 0.4) are used in this simulation. The opening used for this simulation is centered in the middle of the front wall of the compartment fire as shown in Fig. 4. In each simulation, the average temperature is calculated.

One observes a cooling of gas temperature in the compartment especially for large size opening. At the same time, it is found that the reduction of the opening size increases the temperature inside the compartment fire (Fig. 14). Fig. 15 presents the effect of the size of the opening on the total chemical species flow rate (O_2 , N_2 , CO , CO_2 , soot). All of these gases are easily detectable with modern instrumentation. One observes that the mass flux exchanged between the simulated domain and the outside increases with increasing opening size. At the same time, it has been found that the reduction of the size of the opening decreases the total chemical species mass exchanged.

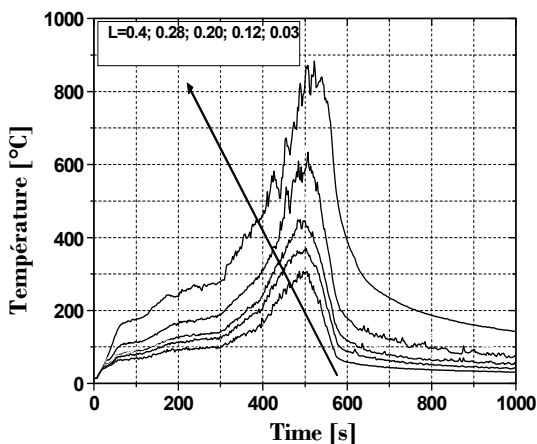


Fig. 14 Effect of the size of the opening on the profile of the mean temperature

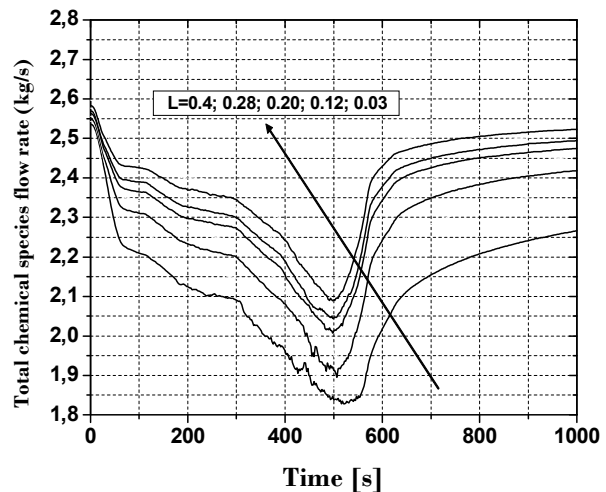


Fig 15 Effect of the size of the opening on the total chemical species flow rate

D. Radiation and Soot

The goal of this section is to study the effect of the fuel used on the production of pollutants. A comparison between five simulations, achieved with FDS and using different types of fuel-oil, e.g. Methane, Propane, Heptane, Wood, and Kerosene allows studying the results sensitivity. These are presented in Figs. 16, 17. Calculations show that the rate of released gases of the methane combustion, reaches weak values of pollutant emissions (CO_2 and CO). This is not the case with other fuels (Propane, Heptane, Kerosene, Wood). The effect of the used fuel nature on carbon monoxide and carbon dioxide emissions is illustrated in Figs. 16, 17.

The carbon monoxide (CO) is a toxic gas associated with incomplete combustion, it's level is relatively low in lean fuel combustion but rises abruptly, as expected, when the mixture becomes rich e.g. burning of wood. Also the yield of CO_2 reaches a maximum value for the same operation. The products of combustion in exhaust stack contain O_2 , CO_2 , CO , NO_x , SO_2 and free water. These gases, particularly CO_2 and SO_2 , start to condensate at temperatures below $135^\circ C$, thus causing the formation of corrosive carbonic acid and sulfuric acid that can corrode the compartment fire. Therefore, methane is chosen in order to reduce the pollutant production. Natural gas, as the cleanest of the fossil fuels, can be used in many ways to help reduction of the emission of pollutants into the atmosphere. Burning natural gas instead of other fossil fuels emits fewer harmful pollutants.

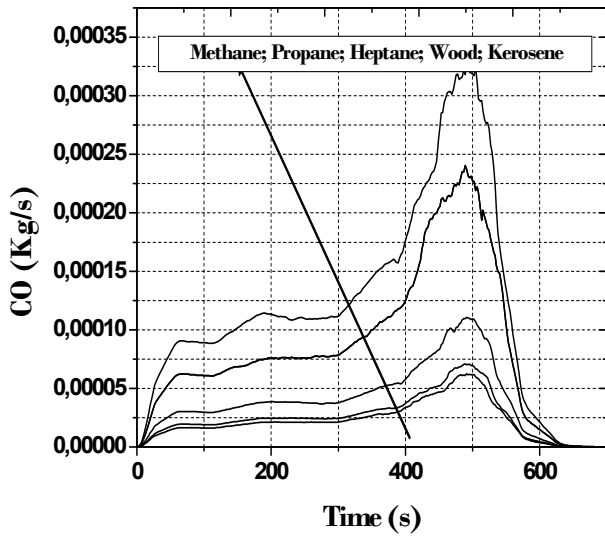
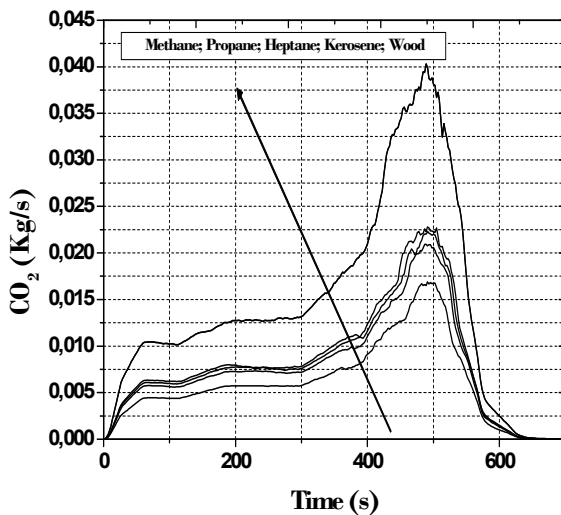


Fig. 16 Carbon oxide CO production

Fig. 17 Carbon dioxide CO₂ production

E. Propagation of Smoke to the Exit of the Compartment Fire

Smoke is the visible suspension in air of solid or liquid particles or gases resulting from combustion or pyrolysis. The nature and concentration of the generated smoke depends on many factors. These include the quantity of the product that is burning, whether the product is flaming or pyrolyzing, the ventilation in the area, and the distance from the fire. Thus, smoke toxicity is not a singular property of a product. A visualization program called "Smokeview" may be used to display the results of FDS simulation. Smokeview is a program that graphically displays smoke propagation. The ability to visualize fire propagation in a 3D building model permits users to obtain the paths that smoke is taking. Fig. 18 shows the propagation of smoke towards the exit of the fire compartment. This smoke contains unburned hydrocarbons, carbon monoxide, carbon dioxide, sulfur oxides, nitrogen

oxides and some particles of soot and all products of combustion. The Smokeview visualization in Figs. 18 (b)-(d) shows that in the interval time between 200 and 400 seconds the smoke becomes denser.

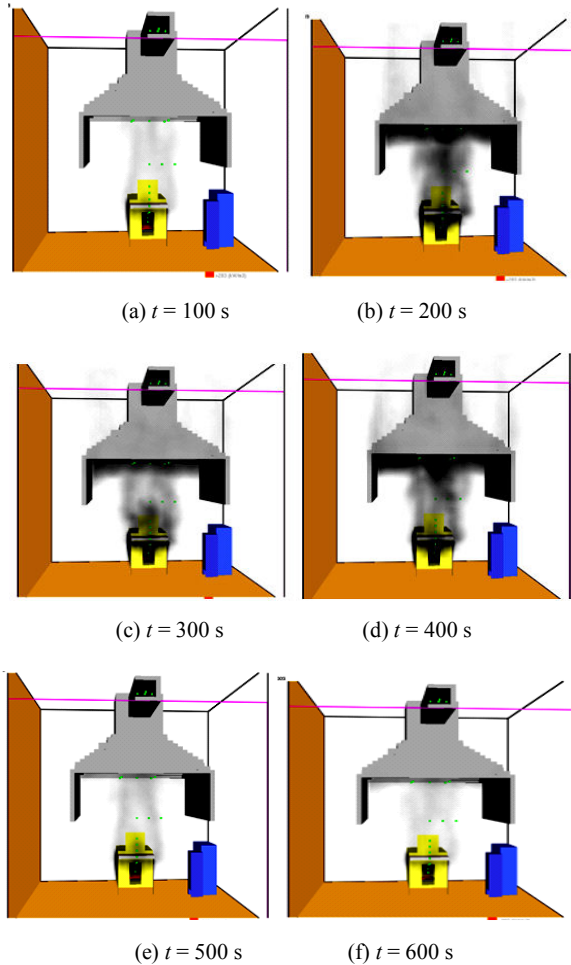


Fig. 18 Propagation of smoke to the exit of the compartment fire

IV. CONCLUSION

Large eddy simulation of the space fire spread and the combustion of the kerosene in a compartment fire are conducted. Based on the comparison of the FDS temperature predictions to the experimental measurements, the following conclusions are made:

- The predictions of the temperature using the FDS code significantly depends on the resolution grid. Good predictions are achieved for cells within the fire compartment smaller than 1/10th of the characteristic fire diameter.
- FDS results are validated with experimental values given in [19]. However, the difference between the experimental results and the FDS predictions may be caused by the soot deposition on the thermocouples.

REFERENCES

- [1] G. Yeoh, R. Yuen, and W. Kwok, "Modelling combustion, radiation and soot processes in compartment fires," *Build Environ*, vol. 38, pp. 593–85, 2003.
- [2] H. you, and G. Faeth, "Turbulent combustion," *Combust Flame*, vol. 38, pp. 261–44, 1982
- [3] B. Morton, "Modeling fires plumes," *Proc 10th International Symposium on Combustion*, pp. 973–982.
- [4] V. Novozhilov, "Computational fluid dynamics modeling of compartment fires," *Proc. Energy. Combust. Sci*, vol. 27, pp. 61–66, 2001.
- [5] E. Zukoski, "Properties of fire plumes," *San Diego-Academic Press*, vol. 50, pp. 4073-4079, 1995.
- [6] V. Novozhilov, B. Moghtaderi, and D. Fletcher, "Computational fluid dynamics modeling of wood combustion," *Fire. Saf*, vol. 27, pp. 69–84, 1996.
- [7] W. Sirignano, "Fuel droplet vaporization and spray combustion theory," *Proc. Energy Combustion*, vol. 9, pp. 291–322, 1983.
- [8] I. Kennedy, "Models of soot formation and oxidation," *Proc. Energy. Combustion*, vol. 23, pp. 95–132, 1997.
- [9] V. Novozhilov, "Validation of fire dynamics simulator (fds) for forced and natural convection flows," *Proc. Energy. Combustion*, Vol. 27, pp. 39–54, 2006.
- [10] U. Köylü, G. Fletcher "Carbon Monoxide and soot emissions from liquid fuel," *Combustion Flame*, vol. 87, pp. 61–76, 1991.
- [11] k. McGrattan, "Fire Dynamic Simulator (Version 4) Technical Reference Guide. *National Institute of standards and Technology*," National Institute of standards and Technology, Special Publication 1018, 2006.
- [12] J. Smagorinsky, "General Circulation Experiments with the Primitive Equations," *Monthly Weather Review*, vol 3, pp. 99–164, 1963.
- [13] B. Merci, "Numerical simulations of full-scale enclosure fires in a small compartment with natural roof ventilation," *Fire. Safety*, vol. 43, pp. 495-511, 2008.
- [14] D. Anderson, J. Tannehill, and R. Pletcher, "Computational Fluid Mechanics and Heat Transfer," *Hemisphere Publishing Corporation*, Philadelphia, 1984.
- [15] K. McGrattan, H. Baum, and R. Rehm, "Fire dynamics simulator user's guide," *National Institute of Standards and Technology*, 2001.
- [16] H. Baum, K. Mcgrattan, and H. Baum, "Simulation of Large Industrial Outdoor Fires," *Proc of the Sixth International Symposium Association for Fire Safety Science*, 2000.
- [17] W. Mell, K. Mcgrattan, and H. Baum, *Proc. Combust*, Vol. 26. pp. 1523–30, 1996.
- [18] C. Huggett, "Estimation of the rate of heat release by means of oxygen consumption measurements," *Fire. Mater*, vol. 4, pp. 61–5., 1980.
- [19] P. Smardz, and V. Novozhilov, "Validation of Fire Dynamics Simulator (FDS) for forced and natural convection flows," *University of Ulster*, October 2006.